JOURNAL OF VIROLOGY, Feb. 2005, p. 1623–1634 Vol. 79, No. 3
0022-538X/05/$08.00+0 doi:10.1128/JVI.79.3.1623–1634.2005

Vaccinia Virus Penetration Requires Cholesterol and Results in Specific Viral Envelope Proteins Associated with Lipid Rafts

Che-Sheng Chung, Cheng-Yen Huang, and Wen Chang*

Institute of Molecular Biology, Academia Sinica, Taipei, Taiwan, Republic of China

Received 29 July 2004/Accepted 20 September 2004

Vaccinia virus infects a wide variety of mammalian cells from different hosts, but the mechanism of virus entry is not clearly defined. The mature intracellular vaccinia virus contains several envelope proteins mediating virion adsorption to cell surface glycosaminoglycans; however, it is not known how the bound virions initiate virion penetration into cells. For this study, we investigated the importance of plasma membrane lipid rafts in the mature intracellular vaccinia virus infection process by using biochemical and fluorescence imaging techniques. A raft-disrupting drug, methyl-β-cyclodextrin, inhibited vaccinia virus uncoating without affecting virion attachment, indicating that cholesterol-containing lipid rafts are essential for virion penetration into mammalian cells. To provide direct evidence of a virus and lipid raft association, we isolated detergent-insoluble glycolipid-enriched membranes from cells immediately after virus infection and demonstrated that several viral envelope proteins, A14, A17L, and D8L, were present in the cell membrane lipid raft fractions, whereas the envelope H3L protein was not. Such an association did not occur after virions attached to cells at 4°C and was only observed when virion penetration occurred at 37°C. Immunofluorescence microscopy also revealed that cell surface staining of viral envelope proteins was colocalized with GM1, a lipid raft marker on the plasma membrane, consistent with biochemical analyses. Finally, mutant viruses lacking the H3L, D8L, or A27L protein remained associated with lipid rafts, indicating that the initial attachment of vaccinia virions through glycosaminoglycans is not required for lipid raft formation.

Virus entry is the first encounter between viruses and host cells. Viruses bind to specific receptors and coreceptors on the plasma membranes of cells to initiate molecular changes that are necessary for cell penetration. Investigations of virus entry into cells are important, not only for understanding the molecular basis of host cell susceptibility, but also for dissecting intracellular early signaling induced by virus infections.

Vaccinia virus is the prototype of the *Orthopoxvirus* genus of the *Poxviridae* family and infects many cell lines and animals (23). Vaccinia virus produces multiple forms of infectious particles, including intracellular mature virus (IMV), intracellular enveloped virus, cell-associated enveloped virus, and extracellular enveloped virus (EEV) (53). The IMV membrane structure is different from that of intracellular enveloped virus, which again is different from those of cell-associated enveloped virus and EEV (84). IMV and EEV were shown to enter cells through different mechanisms (77, 83). The entry of IMV is signaling dependent, but that of EEV is not (44). On the other hand, all forms of vaccinia virus use an A28L-dependent mechanism for cell penetration (72).

IMV represents the majority of infectious progeny produced in cells and contains more than 10 viral envelope proteins on its membrane (38). Previous studies have shown that IMV attaches to cells through binding to cell surface glycosaminoglycans (13). Viral envelope H3L and A27L proteins bind to heparan sulfates, whereas the D8L protein binds to chondroitin sulfates (33, 34, 43). In addition, a monoclonal antibody (MAb) recognizing the L1R protein blocked IMV entry at the postbinding step, suggesting that the L1R protein plays a role in virus penetration (35, 87). Recently, the A28L protein was shown to be essential for vaccinia virus penetration into mammalian cells (71, 72). Although no cellular coreceptor has been identified for vaccinia virus, some data have suggested that cell-bound IMV initiates membrane fusion to deliver viral cores into cells, while other studies have indicated that there is a membrane-shedding mechanism for viral core translocation across the plasma membrane (1, 11, 19, 44, 78, 83). In addition, IMV entry has been shown to trigger cell signaling pathways that involve Rac, MEK, extracellular signal-regulated kinase (ERK), protein kinase A (PKA), and PKC activation, but the molecular mechanism of this activation is currently unknown (18, 41, 44).

The lipid raft hypothesis proposes that cell membranes are organized into distinct cholesterol-rich microdomains that are important for signal transduction, protein sorting, and membrane transport (9, 37, 75, 76). Caveolae, which are specialized lipid raft domains, are plasma membrane invaginations that are abundant in many cell types. Caveolin is the major structural protein of caveolae and is required for invaginated caveola formation.

Recently, lipid rafts on the plasma membrane have been shown to be the portal of entry for many pathogens, including viruses and bacteria (5, 12, 20, 74). In addition, lipid rafts are also involved in cell surface receptor-mediated activation, which requires the aggregation of membrane receptor and adaptor molecules to transmit membrane-proximal signaling into cells (17, 48, 54, 55, 61). Since lipid rafts are rich in sphingolipid and cholesterol, they are more resistant to detergent extraction, which is usually the method of choice to physically separate lipid rafts from other membrane components

* Corresponding author. Mailing address: Institute of Molecular Biology, Academia Sinica, Taipei 11529, Taiwan, Republic of China. Phone: 886-2-2789-9230. Fax: 886-2-2782-6085. E-mail: mbwen@ccvax.sinica.edu.tw.

(30). Methyl-β-cyclodextrin (mβCD) is a derivative of a cyclic oligomer of glucose with a lipophilic property (60). mβCD is known to extract cholesterol out of membranes, disrupt lipid raft formation on cells, and consequently block biological processes that depend on lipid rafts. For this study, we investigated the importance of lipid rafts on the plasma membrane for vaccinia virus IMV entry into mammalian cells by using both biochemical and immunofluorescence analyses. Furthermore, since lipid rafts may serve as a platform for membrane protein aggregation, we also investigated the distribution of viral envelope proteins in the membrane during and immediately after IMV entry.

MATERIALS AND METHODS

Cells, viruses, and reagents. BSC40 cells were maintained in Dulbecco's modified Eagle's medium (DMEM)–10% fetal calf serum. HeLa cells were maintained in DMEM–10% fetal bovine serum. HT-29 cells were obtained from the American Type Culture Collection and were cultured in McCoy's 5A medium–10% fetal bovine serum. L, gro2C, and sog9 cells were obtained from F. Tufaro (3, 28). A wild-type vaccinia virus (WR strain; WT VV) was used for this study. vMJ360, which expresses *lacZ* from a viral early promoter, was obtained from B. Moss (16). A D8L$^-$ mutant virus (v-BssHII) was obtained from E. G. Niles (56). A recombinant vaccinia virus, WR32-7/Ind14K (IA27L), expressing the A27L protein under IPTG (isopropyl-β-D-thiogalactopyranoside) regulation, was obtained from G. L. Smith (66). Rabbit anti-vaccinia IMV (anti-VV), anti-D8L, and anti-H3L sera have been described previously (13, 34, 43). Rabbit anti-L1R and anti-A4L sera were raised against a recombinant L1R protein purified from bacteria. The mouse MAb clone 2D5 recognizing the L1R protein was obtained from Y. Ichihashi (36). Rabbit anti-A14L and anti-A17L-N′ sera were obtained from J. Krijnse Locker (69, 86). A mouse anti-human transferrin receptor (TfR) MAb was purchased from Zymed Laboratories, Inc. A rabbit anti-caveolin Ab was purchased from BD Transduction Laboratories Inc. A tetramethylrhodamine-conjugated goat anti-rabbit Ab was purchased from Molecular Probes Inc. A Cy5-conjugated goat anti-mouse Ab was purchased from Jackson ImmunoResearch Laboratories, Inc. The cholera toxin B subunit conjugated with horseradish peroxidase or fluorescein isothiocyanate (CTB-HRP and CTB-FITC, respectively), mβCD, and water-soluble cholesterol were purchased from Sigma Inc.

Cholesterol depletion and virus entry assays. (i) Cellular cholesterol content measurement. To determine if cholesterol depletion reduces the cellular cholesterol content, we first washed BSC40 cells twice with phosphate-buffered saline (PBS) and then incubated them at 37°C for 1 h with different concentrations of mβCD in DMEM. After two washes with PBS, one set of BSC40 cells were harvested for cholesterol measurement assays with an Amplex Red cholesterol assay kit (Molecular Probes) as described by the manufacturer. In brief, HeLa cells (4×10^6 cells/80 μl of PBS) were lysed by three cycles of freeze-thawing followed by ultrasonication (three bursts of 20 s each at room temperature). Cholesterol was extracted from the cell lysate by the addition of chloroform (200 μl) and methanol (200 μl) to the sonicated lysate (50 μl). The bottom (chloroform) layer was collected and evaporated under a vacuum. The residual cholesterol was dissolved in ethanol (50 μl) and assayed with an Amplex Red cholesterol assay kit (Molecular Probes). For determinations of the percentage of remaining cholesterol after mβCD treatment, the measured fluorescence of treated cells was obtained from a standard curve and divided by the total fluorescence of untreated cells, and the number obtained was multiplied by 100.

(ii) mβCD blocking of vaccinia virus entry. To determine if mβCD reduces vaccinia virus infectivity, we infected BSC40 cells with vMJ360 as described above and cultured them in complete medium for 3 h, fixed them with 0.5% glutaraldehyde, and measured the β-galactosidase (β-Gal) activity expressed from a viral early promoter by X-Gal (5-bromo-4-chloro-3-indolyl-β-D-galactopyranoside) staining as described previously (13). These cells were randomly chosen by microscopy for photography, and the percentage of blue cells was averaged by counting both blue and white cells in at least three photos. The percentage of infection was defined as the percentage of blue cells within the total cell population. When other cell lines such as L and gro2C were tested for virus infection, a multiplicity of infection (MOI) of 5 PFU per cell was also used; however, in the case of sog9 cells, an MOI of 20 PFU per cell was used to ensure that >99% of the cells became infected.

(iii) mβCD blocking of IMV attachment. To determine whether cholesterol depletion affects vaccinia virus IMV attachment to cells, we pretreated BSC40 cells with 10 mM mβCD at 37°C for 1 h, washed them twice with PBS, and subsequently infected them with vaccinia virus at an MOI of 5 PFU per cell at 4°C for 30 min. After washing, the cells were immediately harvested and the amounts of bound virions were determined by plaque assays on BSC40 cells as described previously (34). Alternatively, the infected cells were fixed and bound virion particles were counted after staining with anti-L1R and anti-A4L antibodies by confocal microscopy as described below (83).

(iv) mβCD blocking after virus entry. To determine whether the depletion of cholesterol after virus entry affects viral early gene expression, we infected BSC40 cells with vMJ360 at an MOI of 10 PFU per cell for 30 min at 37°C. After infection, the cells were treated with citrate buffer (40 mM citric acid, 10 mM KCl, 135 mM NaCl, pH 3.0) for exactly 1 min to inactivate bound but unpenetrated virions as described previously (31). After washing, virus-infected cells were incubated with DMEM containing 10 mM mβCD at 37°C for 1 h, washed with PBS, and harvested at 3 h postinfection (p.i.) for use in a β-Gal activity assay using *o*-nitrophenyl-β-D-galactopyranoside as described previously (29).

(v) mβCD toxicity. To determine the toxicity of mβCD, we treated BSC40 cells with various concentrations of mβCD or mock infected the cells. Mock-infected cells were harvested at the same time as the virus-infected cells mentioned above and were stained with trypan blue for cell viability determinations. We used 10 mM mβCD on BSC40 cells for most of the experiments, except for the detergent-resistant membrane isolation experiment, for which we used 5 mM mβCD. Ten millimolar mβCD was also used to treat HeLa, L, gro2C, sog9, and HT-29 cells with little toxicity, consistent with previous reports (73).

(vi) Cholesterol replenishment. For cholesterol replenishment experiments, we followed established protocols as previously described (63). In brief, BSC40 cells were treated with DMEM alone or DMEM containing 10 mM mβCD at 37°C for 1 h. The cells were washed and incubated with DMEM alone or DMEM that was reconstituted with water-soluble cholesterol (400 μg/ml) for another 1 h. The cells were washed again with PBS, infected with vMJ360, and fixed at 3 h p.i. for use in β-Gal assays as described previously (29).

Virion attachment and penetration assays using confocal microscopy. Measurements of cell surface-attached virions and uncoated cores within cells were performed as previously described (72, 83). In brief, HeLa cells were seeded on coverslips at 7×10^4 per well in 12-well plates. Prior to infection, these cells were mock treated, treated with mβCD, or treated with mβCD with cholesterol replenishment as described above. These cells were subsequently infected with vaccinia virus at an MOI of 10 PFU per cell at 4°C for 60 min, washed three times with PBS, and either fixed or incubated at 37°C for 2 h in the presence of cycloheximide (300 μg/ml). The cells were fixed with 4% paraformaldehyde for 5 min at 4°C, followed by incubation for 15 min at room temperature. The cells were then permeabilized in 0.2% saponin–PBS and stained with rabbit anti-A4 serum and a mouse anti-L1R (2D5) antibody, followed by FITC-conjugated goat anti-rabbit and Cy5-conjugated goat anti-mouse antibodies, respectively. DNA was visualized by staining with 4′,6′-diamidino-2-phenylindole dihydrochloride (DAPI; Molecular Probes) (1 μg/ml) in mounting solution. Cell images were collected by confocal laser scanning microscopy with an LSM 5 PASCAL microscope (Carl Zeiss, Gottingen, Germany) using a 63× objective lense. The numbers of fluorescently stained particles were counted from multiple photos, and the average numbers of surface-bound virions and uncoated cores per cell were determined.

Isolation of low-density detergent-insoluble membrane fractions on flotation gradients. Low-density detergent-insoluble membrane microdomains were isolated as described previously, with some modifications (11, 63). HeLa cells (8×10^6) were mock infected or infected with VV at an MOI of 25 PFU per cell for 1 h at 4°C, washed twice with ice-cold PBS to remove unbound virions, and incubated with prewarmed serum-free medium at 37°C. At the indicated time points (0, 15, 30, and 60 min), the cells were scraped with a rubber policeman into ice-cold PBS and pelleted by centrifugation at $200 \times g$ for 3 min at 4°C. The cells were washed with ice-cold PBS and pelleted again. The cell pellet was lysed with 0.3 ml of ice-cold TNE buffer (25 mM Tris [pH 7.5], 150 mM NaCl, 5 mM EDTA) containing 1% Triton X-100 (Merck), 1 mM NaF, and a cocktail of protease inhibitors (Roche). The cells were further incubated at 4°C for 30 min with gentle agitation, and then the cell lysates were centrifuged for 10 min at 3,000 rpm at 4°C in an Eppendorf 5415C centrifuge to remove nuclei and insoluble materials. The precleared supernatants were mixed with equal volumes of 80% (wt/vol) sucrose in TNE buffer and then placed in the bottoms of ultracentrifuge tubes. A discontinuous sucrose gradient was formed by overlaying the homogenates sequentially with 2.1 ml of 30% and 1.3 ml of 5% sucrose in TNE buffer. These mixtures were centrifuged for 18 h at 48,000 rpm at 4°C in an SW60 rotor (Beckman). After centrifugation, the Triton X-100-insoluble, low-density material containing lipid rafts was visible as an opaque band migrating at the boundary between the 5 and 30% sucrose solutions. The gradient fractions

were collected from the top, and a total of 11 fractions (0.36 ml/fraction) were collected and stored at −80°C.

Immunoblot and dot blot analyses. For analyses of the distribution of proteins in the fractions obtained from Triton X-100 flotation experiments, aliquots of 10 μl of each sucrose gradient fraction were mixed with sodium dodecyl sulfate-polyacrylamide gel electrophoresis (SDS-PAGE) sample buffer, and the proteins were resolved by SDS–12% PAGE under denaturing conditions, followed by immunoblotting. In some experiments, the low-density fractions (fractions 4 and 5) from the sucrose gradient were pooled, precipitated with 10% trichloroacetic acid, and solubilized in gel sample buffer prior to separation by SDS–12% PAGE. After transfer, the membranes were blocked with 0.2% I-Block (Applied Biosystems, Inc.) in PBS plus 0.05% Tween 20 at room temperature for 1 h and then incubated with individual primary Abs (anti-caveolin [1:1,000], anti-transferrin receptor [1:1,000], anti-VV [1:1,000], anti-H3L [1:1,000], anti-L1R [1:1,000], anti-A17L-N′ [1:1,000], anti-D8L [1:1,000], and anti-A14L [1:1,000]) at room temperature for 12 h. The membranes were washed and then incubated with secondary antibodies coupled to alkaline phosphatase. The blots were developed with the substrate CDP-Star (Applied Biosystems, Inc.) as described by the manufacturer and then were exposed to film.

For detection of the ganglioside GM1, dot blot analyses were performed as described previously (6). In brief, 50-μl fractions collected from the sucrose gradient were applied to a nitrocellulose membrane in a manifold dot blot apparatus under suction. The membrane was blocked with PBS containing 0.2% I-Block (Applied Biosystems, Inc.) and 0.05% Tween 20 and then incubated with CTB-HRP (0.5 μg/ml) for 30 min. After washing, the fractions containing GM1 were detected by enhanced chemiluminescence (ECL; Amersham) and exposed to an autoradiogram.

Copatching analyses by confocal immunofluorescence microscopy. Copatching analyses of membrane proteins with antibodies were performed as previously described (30, 46). HeLa cells were seeded on round coverslips in 12-well plates. The next day, cells were infected with vaccinia virus at an MOI of 50 PFU per cell in DMEM for 1 h, washed, and transferred to 12°C for patching of lipid rafts. The cells were incubated at 12°C for 1 h with a primary Ab (anti-VV [1:500] or anti-hTfR MAb [1:100]) and CTB-FITC (10 μg/ml) (Sigma Chemical Co.). Subsequently, tetramethylrhodamine-conjugated goat anti-rabbit immunoglobulin G (IgG) (1:500) or Cy5-conjugated goat anti-mouse IgG (1:500) (1.5 mg/ml; Jackson ImmunoResearch Laboratories, Inc.) was added to cells for 30 min. The cells were then fixed for 5 min with 3.7% paraformaldehyde in PBS on ice followed by methanol for 10 min at −20°C, mounted in Vectashield medium (Vector Laboratories, Burlingame, Calif.), and visualized by confocal laser scanning microscopy with an LSM 5 PASCAL instrument (Carl Zeiss) using a 63× objective lenses and accompanying software.

RESULTS

A raft-disrupting agent, mβCD, inhibits vaccinia virus entry. Lipid rafts form microdomains on the plasma membranes of cells and can be disrupted by mβCD, which sequesters cholesterol away from the plasma membrane (60). To test whether mβCD affects vaccinia virus entry, we pretreated BSC40 cells with mβCD for 60 min and infected them with vMJ360, which expresses the *lacZ* gene under the control of an early viral promoter. At 3 h p.i., the cells were fixed and stained for β-Gal expression. As shown in Fig. 1A, the infectivity of vaccinia virus for BSC40 cells was inhibited by mβCD in a dosage-dependent manner, with 50% inhibition at a 2 mM concentration. More than 90% inhibition was achieved with 10 mM mβCD. The reduction in virus infection was not due to any toxic effect of mβCD on BSC40 cells since cell viability was barely affected by mβCD treatment (Fig. 1A). Indeed, a 10 mM mβCD treatment effectively reduced the level of cellular cholesterol by 90% compared to the level found in untreated cells (Fig. 1B). To determine that the inhibition of virus infectivity was not due to any nonspecific effect of mβCD, we replenished the cholesterol in the culture medium after mβCD treatment and monitored the recovery of virus infectivity (Fig. 1C). The addition of cholesterol successfully reversed the inhibitory effect of mβCD on vaccinia virus infection, confirming that the inhibition by the drug was due to its specific sequestering of cholesterol.

In all of our experiments, mβCD was used to pretreat cells and was washed off prior to virus infections. In order to ascertain that the inhibition of virus infection was not due to the inactivation of vaccinia IMV virions per se by mβCD, we collected the washing medium from pretreated cells and incubated it with purified IMV virions at 37°C for 60 min. We found no loss of virion infectivity due to residual mβCD remaining in the washing medium (data not shown). Therefore, our results indicated that cholesterol in plasma membrane microdomains is important for vaccinia virus infection.

To determine if cholesterol extraction specifically affects vaccinia virus entry, we treated cells with mβCD either before or after virus infection and monitored viral early gene expression at 3 h p.i. (Fig. 1D). The results showed that, in contrast to the inhibition caused by cells pretreated with mβCD prior to virus infection (Fig. 1D, mβCD+VV), cholesterol extraction from the cell membrane after vaccinia virus infection did not affect viral early gene expression (Fig. 1D, VV+mβCD), indicating that mβCD blocks vaccinia virus at the entry step. To determine whether mβCD reduces vaccinia virion adsorption to BSC40 cells, we measured the amount of virion binding to mock-treated or mβCD-treated cells (Fig. 1E). The amounts of bound IMV virions on both types of cells were comparable, indicating that cholesterol extraction affects IMV entry at a postbinding step.

To provide direct evidence that mβCD affects virus penetration into cells, we used confocal microscopy with antibodies recognizing the envelope L1R and core A4L proteins to differentiate the surface-bound IMV particles from the penetrated cores inside cells as described previously (Fig. 2) (44, 72, 83). The amounts of bound virions and uncoated cores in cells were also quantitated, and these results are shown in Table 1. As expected, IMV binding to BSC40 cells at 4°C was detected with anti-L1R (19 ± 9 particles/cell) but not anti-A4L antibodies since no virion uncoating occurred at 4°C (Fig. 2A). When the temperature was shifted to 37°C, virion penetration occurred, resulting in the detection of uncoated viral cores with anti-A4L antibodies (20 ± 10 particles/cell) (Fig. 2B). When cells were pretreated with mβCD, the amount of virions binding to cells remained comparable at 4°C (20 ± 5 particles/cell), again confirming that mβCD does not reduce virion attachment to cells (Fig. 2C). However, uncoated cores were hardly detected in the drug-treated cells at 37°C (0.2 ± 0.4 particles/cell), demonstrating that mβCD blocks the virion penetration step (Fig. 2D). The addition of cholesterol did not change virion binding at 4°C (19 ± 6 particles/cell) but successfully reversed the inhibitory effect of mβCD on virus uncoating (16 ± 8 particles/cell) (Fig. 2F), demonstrating that mβCD inhibition of virus penetration was due to its specific sequestering of cholesterol.

Distribution of vaccinia virus envelope proteins on lipid raft microdomains during virus entry. Experimental data with chemical inhibitors such as mβCD are highly suggestive but, nevertheless, are an indirect approach for associating lipid rafts with virus entry. To provide direct evidence for a virion association with lipid rafts during virus entry, we infected cells with vaccinia virus at 4°C for 60 min so that virions attached to

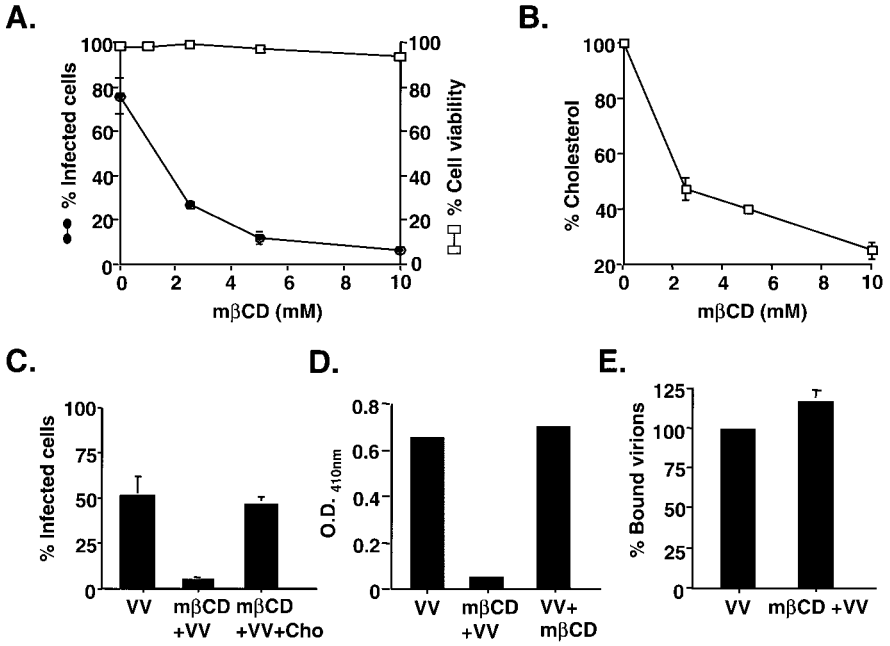

FIG. 1. (A) Vaccinia virus IMV infection is blocked by mβCD. BSC40 cells were pretreated with 0, 2.5, 5, or 10 mM mβCD, subsequently infected with vMJ360, a WT VV expressing *lacZ* from a viral early promoter, at an MOI of 10 PFU per cell, and fixed at 3 h p.i. The beta-galactosidase activity was then determined (filled circles) as described in Materials and Methods (29). In parallel, BSC40 cells were pretreated with various concentrations of mβCD as described above and harvested at the same time as the infected cells, and cell viability was determined by the exclusion of trypan blue dye staining (open squares). (B) Cholesterol levels in cells treated with mβCD. BSC40 cells were treated with various concentrations of mβCD as described above and harvested for cholesterol measurement assays with an Amplex Red cholesterol assay kit (Molecular Probes) as described by the manufacturer. (C) Replenishment of cholesterol rescues viral infection. BSC40 cells were treated with control DMEM and infected with vMJ360 (VV), treated with DMEM plus 10 mM mβCD and infected with vMJ360 (mβCD+VV), or treated with DMEM plus 10 mM mβCD, replenished with cholesterol (400 μg/ml), and infected with vMJ360 (mβCD+VV+Cho) as described in Materials and Methods. The cells were fixed at 3 h p.i. for β-Gal assays. (D) Depletion of cholesterol after virus entry does not affect vaccinia virus early gene expression. BSC40 cells were either treated with medium alone and infected with vMJ360 (VV), pretreated with 10 mM mβCD and subsequently infected with vMJ360 (mβCD+VV), or infected with vMJ360 and subsequently treated with mβCD (VV+mβCD) as described in Materials and Methods. The infected cells were harvested at 3 h p.i. for β-Gal activity assays. (E) Cholesterol depletion does not affect vaccinia virus IMV attachment to cells. BSC40 cells were mock treated or treated with 10 mM mβCD and subsequently infected with WT VV at an MOI of 5 PFU per cell at 4°C for 1 h. After being washed, the cells were immediately harvested and the amounts of bound virions were determined by plaque assays on BSC40 cells as previously described (13).

the cells without penetration. The cells were washed and subsequently shifted to 37°C to initiate membrane fusion and virion penetration. Cell lysates were harvested 0, 15, 30, and 60 min after the temperature shift, and sphingolipid-rich detergent-resistant membranes were isolated by sucrose sedimentation as described in Materials and Methods (Fig. 3). It is well documented that during centrifugation lipid rafts float up to less dense sucrose fractions, as evidenced by the presence of the ganglioside GM1 in fractions 4 and 5 (Fig. 3A) (52). Fractions 4 and 5 were therefore pooled as the raft samples. The bottom fraction 11, which contained the soluble cell lysates, was collected as a nonraft control. The samples were separated by SDS–12% PAGE and analyzed by immunoblot analyses (Fig. 3B). In agreement with all previous reports regarding lipid raft isolation, the raft-associated marker caveolin was detected in pooled fractions 4 and 5 while the nonraft marker transferrin receptor was present in fraction 11 (27). Anti-VV antibodies detected few background bands for mock-infected cells. Interestingly, we did not observe any specific viral protein that was present in the raft fractions from cells that were infected with vaccinia virus at 4°C only, indicating that virion attachment to cells per se does not lead to the viral protein association with lipid rafts. Fifteen minutes after the temperature shift to 37°C, a weak band of 6 to 16 kDa appeared in the raft fraction, and the intensity of this viral protein became prominent 30 and 60 min after the shift to 37°C. Additional minor bands also appeared at the 30- and 60-min time points (Fig. 3B). A purified IMV virion control did not give any signal, confirming that the viral bands observed in raft fractions were not contaminants from comigrating virions. These results thus demonstrated that viral proteins begin associating with lipid rafts during penetration at 37°C. More importantly, since the association of viral proteins with lipid rafts is time and temperature dependent, the results argued against such an association being an artifact occurring post-cell lysis. Although the anti-VV antiserum recognized other cellular and viral proteins in the nonraft fractions, the patterns were different from those observed for the raft fractions.

In order to identify which envelope proteins are associated with lipid rafts, we performed immunoblot analyses with lipid raft fractions, using antibodies that are reactive to individual viral envelope proteins (Fig. 4A). For raft fractions collected from cells infected with WT VV as described for Fig. 3, a moderate staining of the A14L protein was present in lipid

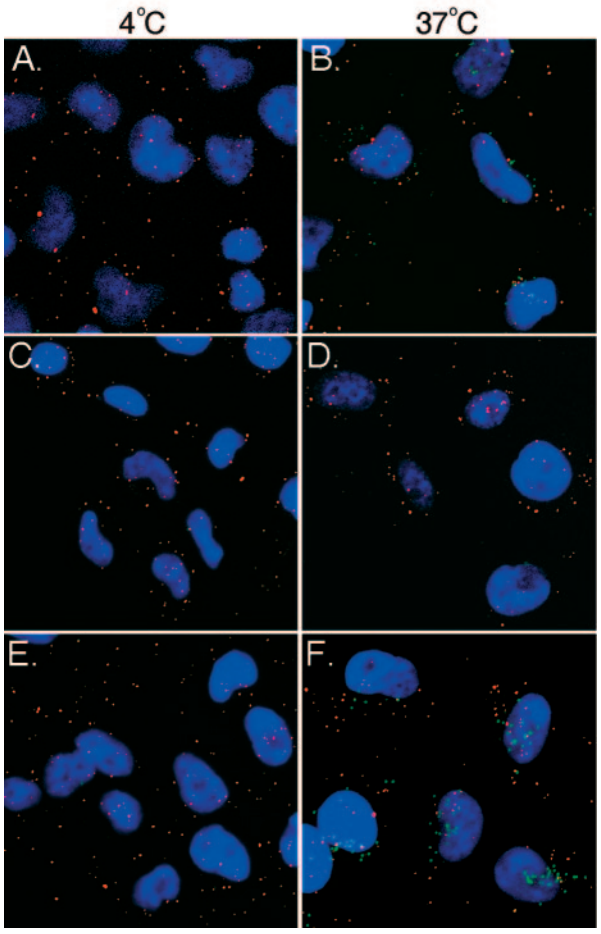

FIG. 2. mβCD blocks vaccinia virus entry at the penetration step. HeLa cells were mock treated (A and B), treated with mβCD (C and D), or treated with mβCD and replenished with cholesterol (E and F) as described above. The cells were subsequently infected with vaccinia virus at an MOI of 10 PFU per cell at 4°C for 60 min, washed three times with PBS, and immediately fixed (A, C, and E) or incubated at 37°C for 2 h in the presence of cycloheximide (300 μg/ml) (B, D, and F). The cells were fixed and doubly stained with rabbit anti-A4 serum and a mouse anti-L1R (2D5) MAb, followed by FITC-conjugated goat anti-rabbit (green) and Cy5-conjugated goat anti-mouse (red) antibodies, respectively. DNA (blue) was visualized by staining with DAPI (Molecular Probes) (1 μg/ml) in mounting solution (72, 83). Cell images were collected as a series of optical sections and then reconstructed as a maximum-intensity projection by confocal laser scanning microscopy with an LSM 5 PASCAL instrument (Carl Zeiss).

rafts as early as 15 min after the shift to 37°C. The amount of raft-associated A14L protein increased significantly 30 and 60 min after the temperature shift. In addition, the amounts of raft-associated A17L and D8L proteins were also increased at the 30- and 60-min time points. In contrast, the H3L protein was not detected in the lipid raft fractions at any time point. Finally, the amount of L1R protein in rafts was minimal but instead increased in the nonraft fraction 30 and 60 min after the shift to 37°C. Antibodies against the vaccinia virus A27L protein did not detect any signal in both raft and nonraft fractions (data not shown). Finally, since the A14L protein is the most abundant raft-associated protein, it was easy to test

TABLE 1. Quantitation of virus entering assay

Virus and treatment	Amt of virus at[a]:	
	4°C	37°C
VV	19 ± 9 (0)	21 ± 9 (20 ± 10)
VV plus mβCD	20 ± 5 (0)	19 ± 6 (0.2 ± 0.4)
VV plus mβCD plus cholesterol	19 ± 6 (0)	24 ± 10 (16 ± 8)

[a] Data show the numbers of Cy5-labeled anti-L1R staining particles per cell, with numbers of FITC-labeled anti-A4L staining particles per cell given in parentheses.

whether mβCD treatment blocked the viral protein association with lipid raft fractions (Fig. 4B). We found that the level of raft-associated A14L protein was greatly reduced in cells that were pretreated with mβCD, indicating that the viral protein association with lipid rafts is regulated by the cholesterol level in cells.

Immunofluorescence detection of viral protein-containing lipid rafts on cell surfaces. To visualize viral proteins associated with lipid rafts on the plasma membrane during virus penetration, we performed confocal immunofluorescence microscopy with HeLa cells. Although lipid raft microdomains were difficult to visualize, this problem was overcome by using antibodies to cross-link raft-associated molecules so that rafts could be detected as fluorescent patches on cell surfaces (27, 30, 55). We therefore infected cells with WT VV and added anti-VV antibodies to show patches of rafts immediately after infection as described in Materials and Methods. As shown in Fig. 4C, patches of viral protein-associated rafts were observed on the surfaces of HeLa cells infected with WT VV. The staining of viral proteins was specific since mock-infected cells did not show any fluorescence (data not shown). Furthermore, the preincubation of HeLa cells with mβCD significantly reduced the extent of patch formation, resulting in dispersed speckles on virus-infected HeLa cells, indicating that the fluorescent patches were formed by mβCD-sensitive rafts.

Because the size and extent of patch formation varied among cells, in order to demonstrate that the patchy staining on these cells indeed represented lipid rafts, we stained the lipid raft marker GM1 on plasma membranes with cholera toxin as described previously (30, 52, 55). Indeed, viral patching signals on HeLa cells infected with WT VV were preferentially colocalized with GM1 staining and not with transferrin receptor, a nonraft marker (Fig. 5A). Furthermore, to confirm that we were not biased toward a particular optical plane for confocal imaging acquisition, we collected *z*-series images from multiple optical sections of these cells (Fig. 5B and C). The colocalization of viral proteins with GM1 was present in all sections throughout the cells, including the apical surface (Fig. 5B), whereas little colocalization of viral proteins with transferrin receptor was observed in all sections (Fig. 5C).

Vaccinia virus association with lipid rafts does not require H3L, A27L, or D8L protein, cell surface glycosaminoglycans, or caveolin. Vaccinia virus contains three glycosaminoglycan (GAG)-binding proteins, namely, H3L, A27L, and D8L (4, 13, 14, 34). Since certain cell surface proteoglycans have been reported to migrate into membrane rafts when bound by large, multivalent ligands, we wondered whether these GAG-binding

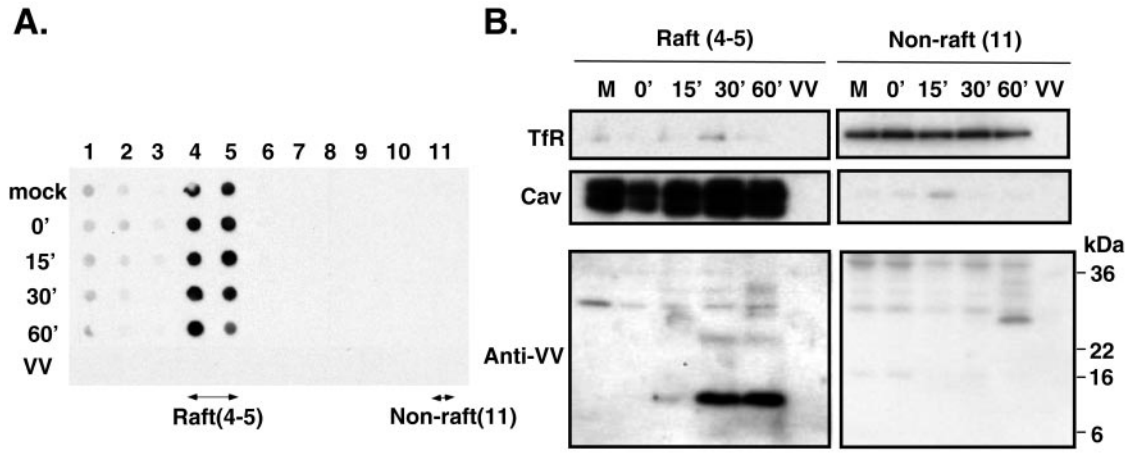

FIG. 3. Vaccinia virus proteins associate with lipid raft fractions during virion penetration. (A) HeLa cells were mock infected or infected with WT VV at an MOI of 25 PFU per cell for 1 h at 4°C, washed, and incubated at 37°C. At the indicated time points (0, 15, 30, and 60 min), cells were harvested and detergent-extracted lysates were prepared. Each cell lysate as well as the detergent-extracted purified vaccinia virus IMV (VV) (10^6 PFU) was placed on top of a sucrose gradient and centrifuged, and 11 fractions were collected from the top to the bottom of the gradient. Aliquots in each fraction were applied to a manifold dot blot apparatus. The fractions containing GM1 were identified by binding to CTB-HRP and were detected by ECL (Amersham) as described previously (6). (B) Immunoblot analyses of raft and nonraft fractions. The lipid raft fractions (4 and 5) and nonraft fractions (11) isolated from infected cells and equivalent fractions (4 and 5) isolated from control IMV shown in panel A were separated by SDS–12% PAGE and transferred to membranes for immunoblot analyses with Abs against transferrin receptor (TfR), caveolin (Cav), or VV. Arrowheads mark raft-associated viral proteins.

proteins of IMV have an additional role in lipid raft association during virus penetration (25, 81). We therefore tested the association of viral proteins with lipid rafts in cells infected with mutant viruses devoid of each of the three GAG-binding envelope proteins, i.e., D8L$^-$, H3L$^-$, and A27L$^-$ mutants, by immunofluorescence microscopy analysis (Fig. 6). The anti-VV antiserum detected viral patches colocalized with GM1 staining on HeLa cells infected with WT VV or the mutant

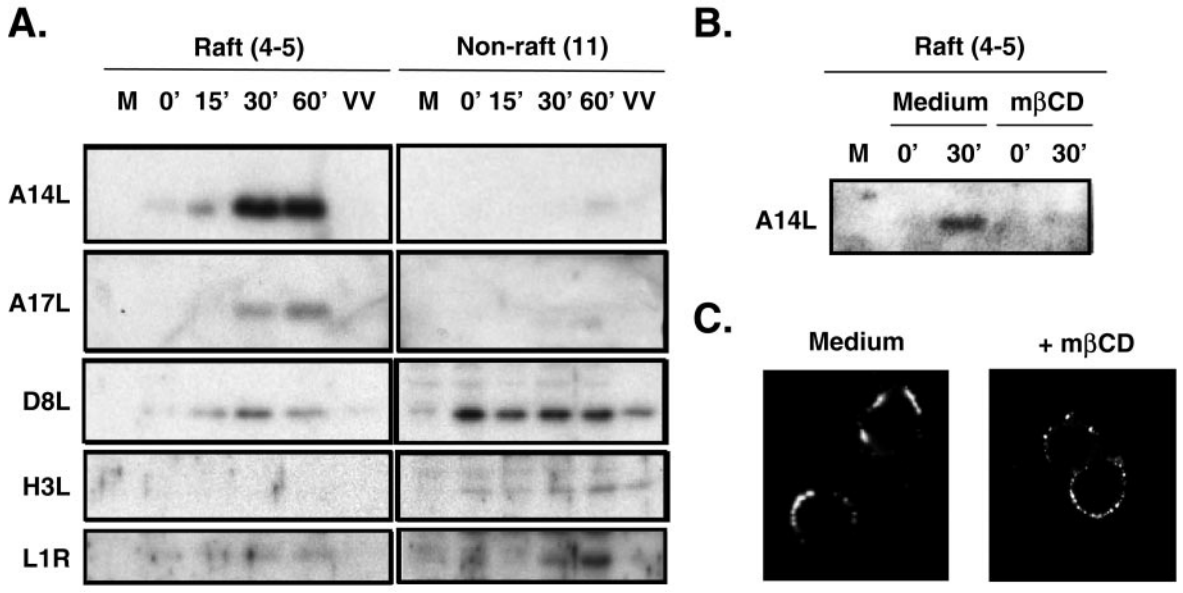

FIG. 4. (A) Identification of viral envelope proteins in lipid rafts. Results are shown for immunoblot analyses of raft (4 and 5) and nonraft (11) fractions isolated from infected HeLa cells as well as equivalent fractions (4 and 5) isolated from control IMV as described in the legend to Fig. 3. These fractions were separated by SDS–12% PAGE and transferred to membranes for immunoblot analyses with various Abs against the A14L, A17L, D8L, H3L, and L1R proteins as described in Materials and Methods. (B) A14L protein in raft fractions is sensitive to mβCD treatment. HeLa cells were pretreated with DMEM only (medium) or DMEM containing mβCD prior to infection with WT VV at 4°C as described in the legend to Fig. 3, cell lysates were collected at 0 and 30 min after a temperature shift to 37°C, and raft fractions were collected for immunoblot analyses with anti-A14L antibodies. (C) Reduction of lipid raft patch formation on plasma membrane by mβCD. HeLa cells were pretreated with DMEM only (medium) or DMEM containing mβCD (+mβCD) and subsequently infected with WT VV at an MOI of 50 PFU per cell in DMEM, washed, and transferred to 12°C for patch formation of lipid rafts by an anti-VV Ab as described in Materials and Methods (30, 46). Samples were fixed, and images were collected by confocal laser scanning microscopy (excitation, 543 nm; emission, 570 nm) (Carl Zeiss).

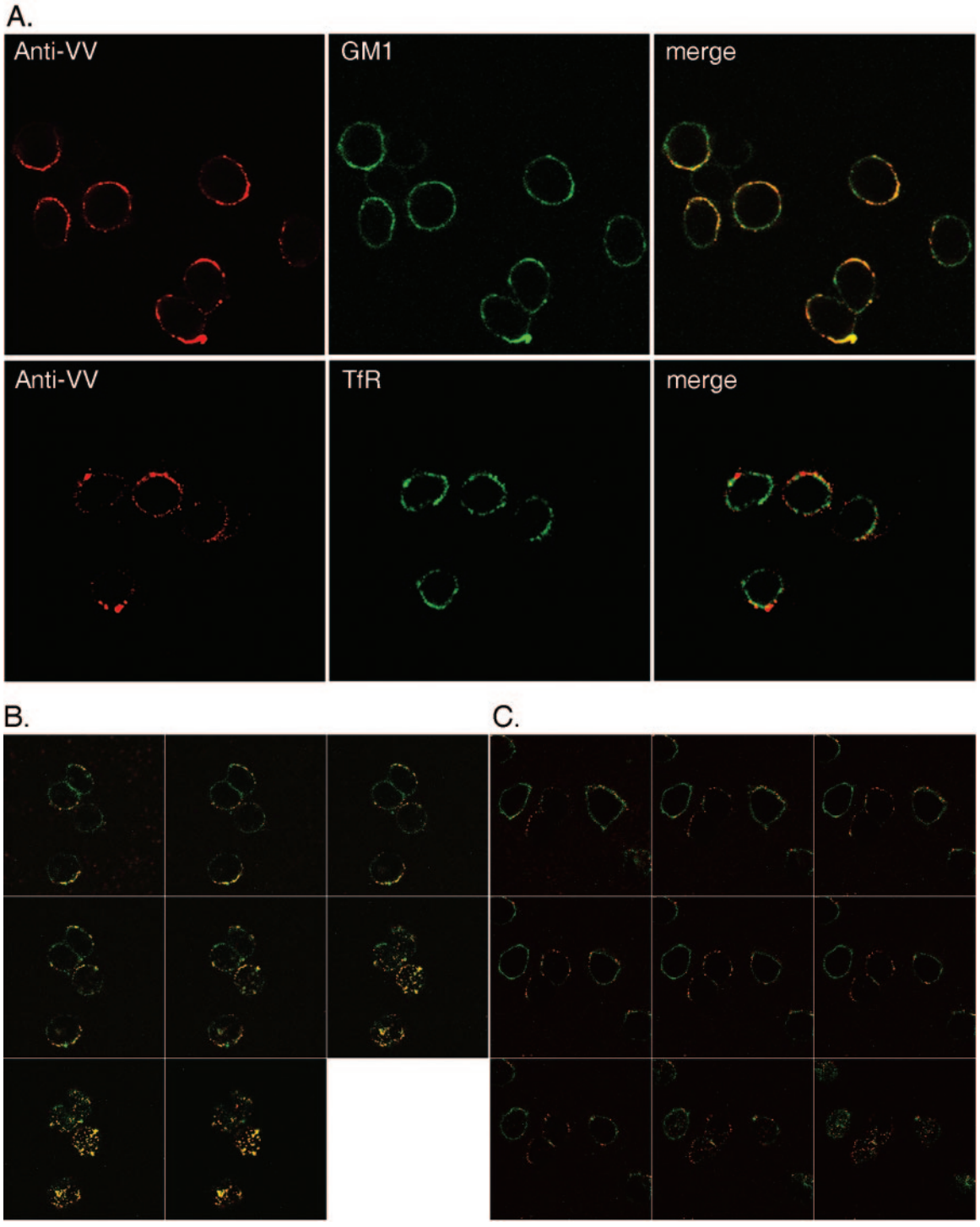

FIG. 5. Viral proteins colocalize with lipid rafts on the plasma membrane. (A) HeLa cells were infected with WT VV at an MOI of 50 PFU per cell and prepared for copatching analyses as described in Materials and Methods. The anti-VV Ab was detected with a rhodamine-conjugated anti-rabbit Ab (red). An anti-TfR MAb and cell surface GM1 were detected with a FITC-conjugated anti-mouse secondary Ab or FITC-CTB (green), respectively. Cells were fixed and visualized by LSM 510 confocal laser scanning microscopy (Carl Zeiss). The stained images were merged to show the colocalization of anti-VV and GM1. (B) Copatching analysis of HeLa cells infected with WT VV as described for panel A with an anti-VV Ab (red) and CTB-FITC (green). A *z*-series of 1-μm-thick optical sections through the entire thickness of the cell was obtained by the use of a 63× objective on a confocal microscope. Only merged stained images are shown here. (C) Copatching analysis of HeLa cells infected with WT VV as described for panel B with an anti-VV Ab (red) and anti-TfR (green). A *z*-series of 1-μm-thick optical sections through the entire thickness of the cell was obtained by the use of a 63× objective on a confocal microscope. Only the merged stained images are shown here.

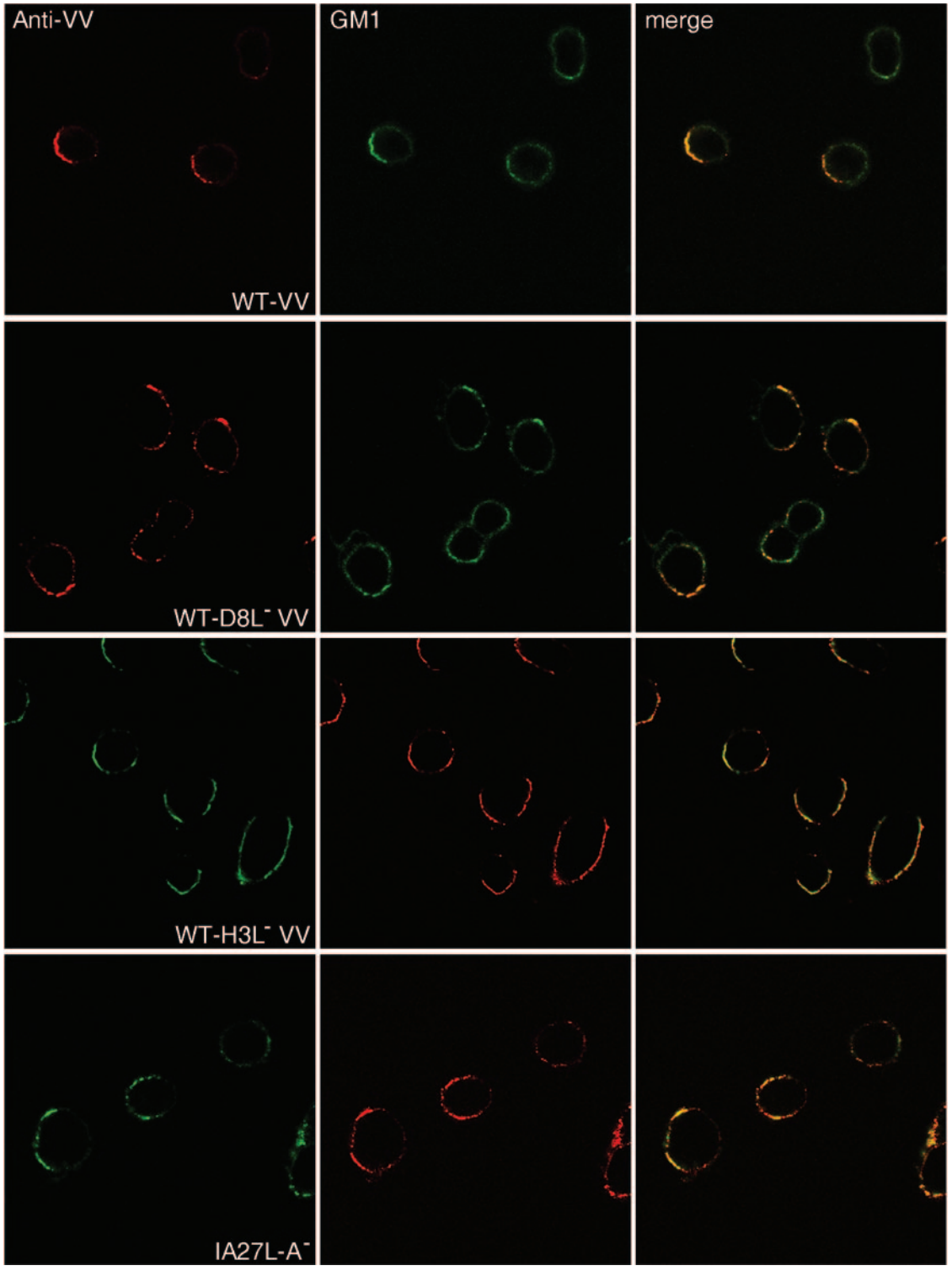

FIG. 6. Copatching analyses of HeLa cells infected with mutant vaccinia viruses defective in expression of the D8L, H3L, or A27L protein by use of an anti-VV Ab (red) and CTB-FITC (green) as described in the legend to Fig. 5A.

viruses, demonstrating that none of these GAG-binding envelope proteins is required for virus targeting to lipid rafts.

We also used GAG-deficient cell lines to clarify the role of cell surface GAGs in lipid raft formation during vaccinia virus entry (Fig. 7A and B). Parental mouse L cells express both heparan sulfates and chondroitin sulfates; gro2C cells are derived from L cells and express only chondroitin sulfates (3, 28). sog9 cells are subsequently derived from gro2C cells and express neither hepa-

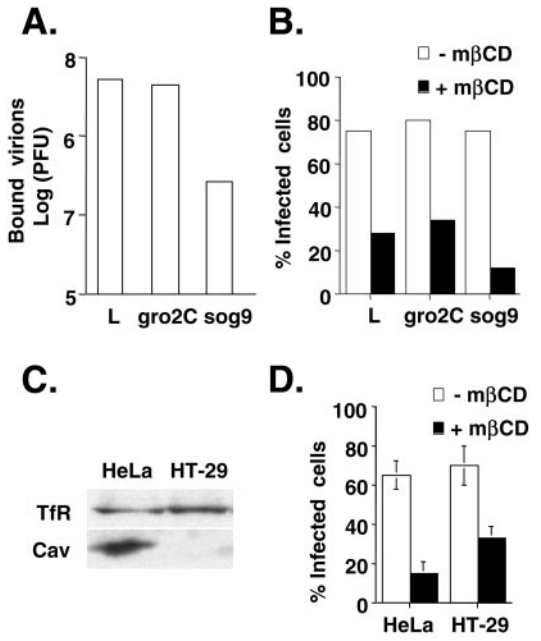

FIG. 7. mβCD blocks WT VV infection in GAG-deficient and caveolin-deficient cells. (A) L, gro2c, and sog9 cells were infected with WT VV at an MOI of 10 at 4°C for 30 min, washed, and then harvested. The amounts of bound IMV were determined by plaque assays with BSC40 cells. (B) Cells were treated with medium alone (−mβCD) or medium containing 10 mM mβCD (+mβCD) and subsequently infected with vMJ360 at an MOI of 5 PFU per cell (for L and gro2 cells) or 20 PFU per cell (for sog9 cells). The cells were fixed at 2 h p.i. and stained with X-Gal, and the numbers of blue cells were counted. The percentage of infected cells = 100 × [(number of blue cells)/(number of blue cells + number of white cells)]. (C) Immunoblots of HeLa and HT-29 cell lysates with anti-transferrin or anti-caveolin Ab. (D) HeLa and HT-29 cells were treated with medium alone (−mβCD) or medium containing 10 mM mβCD (+mβCD) and subsequently infected with vMJ360 at an MOI of 10 PFU per cell. Viral early gene expression was determined by a β-Gal staining assay as described for panel B.

ran sulfates nor chondroitin sulfates (3, 28). The binding of WT VV to L and gro2C cells was comparable, whereas the amount of virions bound to sog9 cells was significantly reduced, confirming that cell surface GAGs are important for the virion attachment step (Fig. 6A). However, despite its low binding efficiency, penetration of the bound IMV into sog9 cells remained sensitive to mβCD, indicating that IMV attachment to cell surface GAGs is independent of lipid raft formation (Fig. 6B).

Finally, lipid rafts on the plasma membrane contain caveolin, which was shown to be essential for caveola-mediated endocytosis (40, 58, 59). We obtained a cell line, HT-29, which is defective for caveolin expression and consequently unable to form caveolae (Fig. 7C) (79). When HT-29 cells were infected with WT VV in the presence of mβCD, virus entry into the cells was inhibited (Fig. 7D). We therefore concluded that lipid raft formation remains critical for vaccinia virus entry while being independent of GAG attachment and caveola formation.

DISCUSSION

Lipid rafts exist on the plasma membrane and in intracellular organelles and are different in their composition, physical properties, and biological functions (9, 12, 26, 37). This study has established that vaccinia virus IMV associates with lipid rafts on plasma membranes during and immediately after virus penetration. Firstly, we showed that mβCD inhibited cholesterol-mediated virus penetration into cells without interference with virion attachment on cell surfaces. Secondly, we showed by the use of biochemical fractionation that the A14L, A17L, and D8L viral envelope proteins were partitioned in lipid rafts during virus penetration and, at least for the A14L protein, that such an association requires cholesterol. Thirdly, the copatching of viral proteins with GM1, but not transferrin receptor, on the cell surface was demonstrated by confocal microscopy. Using a combination of these approaches, we concluded that vaccinia virus IMV utilizes cholesterol-containing lipid rafts on plasma membranes for virion penetration into cells.

Lipid rafts are rich in cholesterol, whose intercalation into membrane lipid rafts generates high-curvature membrane structures (21). The extraction of cholesterol by mβCD inhibits the entry of many viruses, including human immunodeficiency virus (HIV), poliovirus, Ebola virus, herpesvirus, influenza virus, and rotavirus (5, 6, 15, 62, 70, 80). The drug may block virus entry by eliminating a membrane distortion that otherwise facilitates efficient membrane fusion or caveola-mediated endocytosis. However, vesicular stomatitis virus entry is not affected by mβCD treatment, indicating that the inhibitory effect of mβCD is not simply due to a drastic alteration in the cell membrane (6, 15).

Regarding the role of lipid rafts in vaccinia virus penetration, we believe that lipid rafts facilitate membrane fusion rather than caveola-mediated endocytosis for vaccinia virus IMV based on the following rationale. First of all, previous data showed that the vaccinia virus IMV envelope fuses with cell membranes during vaccinia virus entry into cells (19). Meanwhile, the average size of caveolae on the plasma membrane is 50 to 100 nm, which is large enough for the endocytosis of echovirus and simian virus 40 virus but possibly too small for vaccinia virus IMV (47, 57, 59). Moreover, cell fusion from within and from without was blocked by mβCD, supporting the hypothesis that lipid rafts are critical for membrane fusion (data not shown). Finally, HT-29 cells, a cell line expressing no caveolin, are readily infected by vaccinia virus, indicating that vaccinia virus entry does not require caveolin-1-mediated caveola formation. Although other less defined processes such as macropinocytosis cannot be ruled out, our data are most consistent with the conclusion that lipid rafts create a platform to facilitate vaccinia virus fusion with cells. Our data also revealed that although cell surface GAGs are important for the recruitment of abundant IMV virions for cell attachment, they are not essential for subsequent lipid raft association, indicating that additional viral proteins and cell interactions regulate such an association.

In this study, we identified several envelope proteins, i.e., the A14L, A17L, and D8L proteins, which are present in lipid rafts during virus penetration. The A14L and A17L proteins were more exclusively found in lipid rafts, whereas the D8L protein was present in both raft and nonraft fractions. One may postulate that some of these proteins are involved in virus penetration whereas others may associate with rafts as a consequence of viral and cellular membrane fusion. In the case of

the latter, they might participate in lipid raft stabilization to augment subsequent signaling events. It was somewhat unexpected that the L1R protein was more present in nonraft fractions since a role in virion penetration has been postulated for this protein based on neutralizing Ab experiments in the literature (35, 36, 87). It will be interesting to find out whether the vaccinia virus A28L protein, whose presence on IMV is essential for virion penetration, is associated or not associated with rafts (71, 72). We suspect that there are other unidentified viral and/or cellular proteins present in the isolated lipid rafts, although the actual numbers of these proteins are difficult to obtain due to the lack of specific Abs to recognize individual proteins in immunoblot analyses. For example, if vaccinia virus IMV binds to a coreceptor for cell entry, it is possible that such a molecule would be present in lipid rafts, as reported for the coxsackievirus and adenovirus receptor for coxsackievirus B, CXCR4 for HIV, and CAT1 for murine leukemia virus (2, 45, 55). How to identify these raft-associated proteins without bias becomes increasingly important. To solve the limitation of Abs and to facilitate novel protein identification, we are currently developing a proteomic approach to determine lipid raft-associated viral and cellular proteins by mass spectrometry (24).

The structural requirements for proteins targeting lipid rafts are not immediately evident from the literature. Our data showed that the distribution of the A14L and A17L proteins in membranes is more raft specific than that of the D8L protein. The difference may be due to technical reasons, such as the detergent concentration, that dissociate weaker lipid-protein interactions. While we do not know its underlying mechanism, this heterogeneous nature of viral protein distribution in rafts appears more common than we expected since a recent study with pseudorabies virus also showed a similar situation, i.e., more gB in rafts, gE in both raft and nonraft fractions, and gC and gD mainly in nonraft fractions (22).

The topology of some vaccinia virus proteins is known but does not necessarily explain their preference for raft association. For example, both the D8L and H3L proteins are type 1 integral membrane proteins of IMV; however, only the former was detected in lipid rafts. This finding is similar to that from a recent study of herpes simplex virus gB and gC, two heparan sulfate-binding virion proteins, in which only gB was retained in lipid rafts during herpes simplex virus entry (6). The A17L protein contains two transmembrane regions, with the N terminus exposed on the surfaces of IMV particles and the C terminus embedded in the viral membranes (7, 39, 86). The A14L protein also spans the membrane twice, but the protein is embedded within the virion inner membranes and is not accessible to protease digestion (69). None of these viral proteins contain homologous motifs to explain their association with lipid rafts. It is likely that some of the proteins may be associated with lipid rafts due to the aggregation of protein complexes through protein-protein interactions, but how this is achieved is not known. So far, only an interaction between the A14L and A17L proteins has been reported, and no information regarding the D8L protein forming a complex with another protein has been reported (67).

Lipid modification of the A14L protein may be an interesting and relevant subject to explore with regards to raft association. Previous studies revealed that the A14L protein was labeled with [^{3}H]myristic acid in virus-infected cells, although the precise residue of myristoylation has not been published (67). Myristoylated proteins are commonly associated with diverse membranes, and the targeting specificity and membrane affinity of a myristoylated protein might also be enhanced by other factors, such as a nearby palmitoylation site, transmembrane region, or protein-protein interaction (49, 88). The involvement of myristoyl anchors in virus entry has been investigated (49). Myristoylation of the hepatitis B virus large S antigen is required for virus infectivity in vitro (10). Myristoylation of the reovirus μ1 structural protein is important for insertion into the host cell membrane (42). Myristoylation of the A14L protein may not be the only signal for raft targeting, as another myristoylated envelope protein, L1R, was not preferentially found in rafts. Whether myristoylation, along with other structural features, serves as a target signal to anchor the A14L protein to lipid rafts on the plasma membrane remains to be determined. Finally, the raft association of viral envelope proteins may occur indirectly through receptor-protein aggregation in response to phosphorylation regulation. Viral A14L and A17L proteins both contain residues that may be phosphorylated in vivo, and the effect of phosphorylation on their association with rafts will be investigated in the future (8, 50, 67, 68, 82).

Although vaccinia virus IMV binding requires cell surface GAGs, this study showed that virion fusion and penetration into cells require cholesterol-containing lipid rafts. However, the significance of lipid rafts goes beyond their being treated simply as biochemical constituents of the plasma membrane. Lipid rafts are important because they also serve as signal-sensing centers for cells when they are activated by ligand-receptor interactions or chemical treatment or challenged by pathogen invasion (40). The initiation and propagation of signaling in immune cells occur in lipid rafts (32, 85). Gangliosides in lipid rafts bind to growth factor receptors to mediate mitogenic signaling (51). To this end, it is interesting that previous work has indicated that the binding of vaccinia virus IMV to CHO cells is sufficient to trigger apoptotic signaling (64). The dissection of lipid raft components will provide a molecular basis to investigate IMV-induced apoptotic signaling. Furthermore, lipid rafts may provide the physical means to converge kinase signaling and cytoskeleton rearrangements that are necessary for core transport inside cells. It remains to be determined whether Rac activation and PKA/PKC signaling are induced upon lipid raft formation (18, 41, 44). In the future, it will be interesting to isolate biochemical complexes from lipid rafts and to analyze virus-induced clustering of signaling molecules through lipid raft formation.

ACKNOWLEDGMENTS

We thank Y. Ichihashi for reading the manuscript and for helpful suggestions.

This work was supported by grants from Academia Sinica (AC5202401023-2) and the National Science Council (NSC92-2311-B-001-043) of the Republic of China.

REFERENCES

1. **Armstrong, J. A., D. H. Metz, and M. R. Young.** 1973. The mode of entry of vaccinia virus into L cells. J. Gen. Virol. **21:**533–537.
2. **Ashbourne Excoffon, K. J., T. Moninger, and J. Zabner.** 2003. The coxsackie B virus and adenovirus receptor resides in a distinct membrane microdomain. J. Virol. **77:**2559–2567.
3. **Banfield, B. W., Y. Leduc, L. Esford, K. Schubert, and F. Tufaro.** 1995.

Sequential isolation of proteoglycan synthesis mutants by using herpes simplex virus as a selective agent: evidence for a proteoglycan-independent virus entry pathway. J. Virol. **69:**3290–3298.
4. **Barman, S., and D. P. Nayak.** 2000. Analysis of the transmembrane domain of influenza virus neuraminidase, a type II transmembrane glycoprotein, for apical sorting and raft association. J. Virol. **74:**6538–6545.
5. **Bavari, S., C. M. Bosio, E. Wiegand, G. Ruthel, A. B. Will, T. W. Geisbert, M. Hevey, C. Schmaljohn, A. Schmaljohn, and M. J. Aman.** 2002. Lipid raft microdomains: a gateway for compartmentalized trafficking of Ebola and Marburg viruses. J. Exp. Med. **195:**593–602.
6. **Bender, F. C., J. C. Whitbeck, M. Ponce de Leon, H. Lou, R. J. Eisenberg, and G. H. Cohen.** 2003. Specific association of glycoprotein B with lipid rafts during herpes simplex virus entry. J. Virol. **77:**9542–9552.
7. **Betakova, T., E. J. Wolffe, and B. Moss.** 1999. Membrane topology of the vaccinia virus A17L envelope protein. Virology **261:**347–356.
8. **Betakova, T., E. J. Wolffe, and B. Moss.** 1999. Regulation of vaccinia virus morphogenesis: phosphorylation of the A14L and A17L membrane proteins and C-terminal truncation of the A17L protein are dependent on the F10L kinase. J. Virol. **73:**3534–3543.
9. **Brown, D. A., and E. London.** 1998. Functions of lipid rafts in biological membranes. Annu. Rev. Cell Dev. Biol. **14:**111–136.
10. **Bruss, V., J. Hagelstein, E. Gerhardt, and P. R. Galle.** 1996. Myristylation of the large surface protein is required for hepatitis B virus in vitro infectivity. Virology **218:**396–399.
11. **Chang, A., and D. H. Metz.** 1976. Further investigations on the mode of entry of vaccinia virus into cells. J. Gen. Virol. **32:**275–282.
12. **Chazal, N., and D. Gerlier.** 2003. Virus entry, assembly, budding, and membrane rafts. Microbiol. Mol. Biol. Rev. **67:**226–237.
13. **Chung, C. S., J. C. Hsiao, Y. S. Chang, and W. Chang.** 1998. A27L protein mediates vaccinia virus interaction with cell surface heparan sulfate. J. Virol. **72:**1577–1585.
14. **da Fonseca, F. G., E. J. Wolffe, A. Weisberg, and B. Moss.** 2000. Effects of deletion or stringent repression of the H3L envelope gene on vaccinia virus replication. J. Virol. **74:**7518–7528.
15. **Danthi, P., and M. Chow.** 2004. Cholesterol removal by methyl-beta-cyclodextrin inhibits poliovirus entry. J. Virol. **78:**33–41.
16. **Davison, A. J., and B. Moss.** 1989. Structure of vaccinia virus early promoters. J. Mol. Biol. **210:**749–769.
17. **del Pozo, M. A., N. B. Alderson, W. B. Kiosses, H. H. Chiang, R. G. Anderson, and M. A. Schwartz.** 2004. Integrins regulate Rac targeting by internalization of membrane domains. Science **303:**839–842.
18. **de Magalhaes, J. C., A. A. Andrade, P. N. Silva, L. P. Sousa, C. Ropert, P. C. Ferreira, E. G. Kroon, R. T. Gazzinelli, and C. A. Bonjardim.** 2001. A mitogenic signal triggered at an early stage of vaccinia virus infection: implication of MEK/ERK and protein kinase A in virus multiplication. J. Biol. Chem. **276:**38353–38360.
19. **Doms, R. W., R. Blumenthal, and B. Moss.** 1990. Fusion of intra- and extracellular forms of vaccinia virus with the cell membrane. J. Virol. **64:**4884–4892.
20. **Duncan, M. J., J. S. Shin, and S. N. Abraham.** 2002. Microbial entry through caveolae: variations on a theme. Cell Microbiol. **4:**783–791.
21. **Farsad, K., and P. De Camilli.** 2003. Mechanisms of membrane deformation. Curr. Opin. Cell Biol. **15:**372–381.
22. **Favoreel, H. W., T. C. Mettenleiter, and H. J. Nauwynck.** 2004. Copatching and lipid raft association of different viral glycoproteins expressed on the surfaces of pseudorabies virus-infected cells. J. Virol. **78:**5279–5287.
23. **Fenner, F.** 1990. Poxviruses, p. 2113–2133. *In* B. Fields and D. M. Knipe (ed.), Fields virology. Raven Press, New York, N.Y.
24. **Foster, L. J., C. L. De Hoog, and M. Mann.** 2003. Unbiased quantitative proteomics of lipid rafts reveals high specificity for signaling factors. Proc. Natl. Acad. Sci. USA **100:**5813–5818.
25. **Fuki, I. V., M. E. Meyer, and K. J. Williams.** 2000. Transmembrane and cytoplasmic domains of syndecan mediate a multi-step endocytic pathway involving detergent-insoluble membrane rafts. Biochem J. **35:**607–612.
26. **Gaus, K., E. Gratton, E. P. Kable, A. S. Jones, I. Gelissen, L. Kritharides, and W. Jessup.** 2003. Visualizing lipid structure and raft domains in living cells with two-photon microscopy. Proc. Natl. Acad. Sci. USA **100:**15554–15559.
27. **Gomez-Mouton, C., J. L. Abad, E. Mira, R. A. Lacalle, E. Gallardo, S. Jimenez-Baranda, I. Illa, A. Bernad, S. Manes, and A. C. Martinez.** 2001. Segregation of leading-edge and uropod components into specific lipid rafts during T cell polarization. Proc. Natl. Acad. Sci. USA **98:**9642–9647.
28. **Gruenheid, S., L. Gatzke, H. Meadows, and F. Tufaro.** 1993. Herpes simplex virus infection and propagation in a mouse L cell mutant lacking heparan sulfate proteoglycans. J. Virol. **67:**93–100.
29. **Guarente, L., and M. Ptashne.** 1981. Fusion of *Escherichia coli lacZ* to the cytochrome c gene of *Saccharomyces cerevisiae*. Proc. Natl. Acad. Sci. USA **78:**2199–2203.
30. **Harder, T., P. Scheiffele, P. Verkade, and K. Simons.** 1998. Lipid domain structure of the plasma membrane revealed by patching of membrane components. J. Cell Biol. **141:**929–942.
31. **Highlander, S. L., S. L. Sutherland, P. J. Gage, D. C. Johnson, M. Levine, and J. C. Glorioso.** 1987. Neutralizing monoclonal antibodies specific for herpes simplex virus glycoprotein D inhibit virus penetration. J. Virol. **61:**3356–3364.
32. **Holowka, D., and B. Baird.** 2001. Fc(epsilon)RI as a paradigm for a lipid raft-dependent receptor in hematopoietic cells. Semin. Immunol. **13:**99–105.
33. **Hsiao, J.-C., C.-S. Chung, and W. Chang.** 1998. Cell surface proteoglycans are necessary for A27L protein-mediated cell fusion: identification of the N-terminal region of A27L protein as the glycosaminoglycan-binding domain. J. Virol. **72:**8374–8379.
34. **Hsiao, J.-C., C.-S. Chung, and W. Chang.** 1999. Vaccinia virus envelope D8L protein binds to cell surface chondroitin sulfate and mediates the adsorption of intracellular mature virions to cells. J. Virol. **73:**8750–8761.
35. **Ichihashi, Y., and M. Oie.** 1996. Neutralizing epitope on penetration protein of vaccinia virus. Virology **220:**491–494.
36. **Ichihashi, Y., T. Takahashi, and M. Oie.** 1994. Identification of a vaccinia virus penetration protein. Virology **202:**834–843.
37. **Ikonen, E.** 2001. Roles of lipid rafts in membrane transport. Curr. Opin. Cell Biol. **13:**470–477.
38. **Jensen, O. N., T. Houthaeve, A. Shevchenko, S. Cudmore, T. Ashford, M. Mann, G. Griffiths, and J. Krijnse Locker.** 1996. Identification of the major membrane and core proteins of vaccinia virus by two-dimensional electrophoresis. J. Virol. **70:**7485–7497.
39. **Krijnse-Locker, J., S. Schleich, D. Rodriguez, B. Goud, E. J. Snijder, and G. Griffiths.** 1996. The role of a 21-kDa viral membrane protein in the assembly of vaccinia virus from the intermediate compartment. J. Biol. Chem. **271:**14950–14958.
40. **Kurzchalia, T. V., and R. G. Parton.** 1999. Membrane microdomains and caveolae. Curr. Opin. Cell Biol. **11:**424–431.
41. **Leao-Ferreira, L. R., R. Paes-De-Carvalho, F. G. De Mello, and N. Moussatche.** 2002. Inhibition of vaccinia virus replication by adenosine in BSC-40 cells: involvement of A(2) receptor-mediated PKA activation. Arch. Virol. **147:**1407–1423.
42. **Liemann, S., K. Chandran, T. S. Baker, M. L. Nibert, and S. C. Harrison.** 2002. Structure of the reovirus membrane-penetration protein, Mu1, in a complex with is protector protein, Sigma3. Cell **108:**283–295.
43. **Lin, C. L., C. S. Chung, H. G. Heine, and W. Chang.** 2000. Vaccinia virus envelope H3L protein binds to cell surface heparan sulfate and is important for intracellular mature virion morphogenesis and virus infection in vitro and in vivo. J. Virol. **74:**3353–3365.
44. **Locker, J. K., A. Kuehn, S. Schleich, G. Rutter, H. Hohenberg, R. Wepf, and G. Griffiths.** 2000. Entry of the two infectious forms of vaccinia virus at the plasma membrane is signaling-dependent for the IMV but not the EEV. Mol. Biol. Cell **11:**2497–2511.
45. **Lu, X., and J. Silver.** 2000. Ecotropic murine leukemia virus receptor is physically associated with caveolin and membrane rafts. Virology **276:**251–258.
46. **Manes, S., G. del Real, R. A. Lacalle, P. Lucas, C. Gomez-Mouton, S. Sanchez-Palomino, R. Delgado, J. Alcami, E. Mira, and A. C. Martinez.** 2000. Membrane raft microdomains mediate lateral assemblies required for HIV-1 infection. EMBO Rep. **1:**190–196.
47. **Marjomaki, V., V. Pietiainen, H. Matilainen, P. Upla, J. Ivaska, L. Nissinen, H. Reunanen, P. Huttunen, T. Hyypia, and J. Heino.** 2002. Internalization of echovirus 1 in caveolae. J. Virol. **76:**1856–1865.
48. **Marmor, M. D., and M. Julius.** 2001. Role for lipid rafts in regulating interleukin-2 receptor signaling. Blood **98:**1489–1497.
49. **Maurer-Stroh, S., and F. Eisenhaber.** 2004. Myristoylation of viral and bacterial proteins. Trends Microbiol. **12:**178–185.
50. **Mercer, J., and P. Traktman.** 2003. Investigation of structural and functional motifs within the vaccinia virus A14 phosphoprotein, an essential component of the virion membrane. J. Virol. **77:**8857–8871.
51. **Miljan, E. A., and E. G. Bremer.** 2002. Regulation of growth factor receptors by gangliosides. Sci. STKE **2002:**RE15.
52. **Montecucco, C., E. Papini, and G. Schiavo.** 1994. Bacterial protein toxins penetrate cells via a four-step mechanism. FEBS Lett. **346:**92–98.
53. **Moss, B.** 2001. *Poxviridae*: the viruses and their replication, p. 2849–2883. *In* D. M. Knipe et al. (ed.), Fields virology. Lippincott Williams & Wilkins, Philadelphia, Pa.
54. **Muppidi, J. R., and R. M. Siegel.** 2004. Ligand-independent redistribution of Fas (CD95) into lipid rafts mediates clonotypic T cell death. Nat. Immunol. **5:**182–189.
55. **Nguyen, D. H., and D. Taub.** 2002. CXCR4 function requires membrane cholesterol: implications for HIV infection. J. Immunol. **168:**4121–4126.
56. **Niles, E. G., and J. Seto.** 1988. Vaccinia virus gene D8 encodes a virion transmembrane protein. J. Virol. **62:**3772–3778.
57. **Norkin, L. C.** 1999. Simian virus 40 infection via MHC class I molecules and caveolae. Immunol. Rev. **168:**13–22.
58. **Pelkmans, L., and A. Helenius.** 2003. Insider information: what viruses tell us about endocytosis. Curr. Opin. Cell Biol. **15:**414–422.
59. **Pelkmans, L., J. Kartenbeck, and A. Helenius.** 2001. Caveolar endocytosis of simian virus 40 reveals a new two-step vesicular-transport pathway to the ER. Nat. Cell Biol. **3:**473–483.

60. **Pitha, J., T. Irie, P. B. Sklar, and J. S. Nye.** 1988. Drug solubilizers to aid pharmacologists: amorphous cyclodextrin derivatives. Life Sci. **43:**493–502.
61. **Pizzo, P., E. Giurisato, A. Bigsten, M. Tassi, R. Tavano, A. Shaw, and A. Viola.** 2004. Physiological T cell activation starts and propagates in lipid rafts. Immunol. Lett. **91:**3–9.
62. **Popik, W., and T. M. Alce.** 2004. CD4 receptor localized to nonraft membrane microdomains supports HIV-1 entry. Identification of a novel raft localization marker in CD4. J. Biol. Chem. **279:**704–712.
63. **Popik, W., T. M. Alce, and W. C. Au.** 2002. Human immunodeficiency virus type 1 uses lipid raft-colocalized CD4 and chemokine receptors for productive entry into $CD4^+$ T cells. J. Virol. **76:**4709–4722.
64. **Ramsey-Ewing, A., and B. Moss.** 1998. Apoptosis induced by a postbinding step of vaccinia virus entry into Chinese hamster ovary cells. Virology **242:** 138–149.
65. **Rodriguez, D., J. R. Rodriguez, and M. Esteban.** 1993. The vaccinia virus 14-kilodalton fusion protein forms a stable complex with the processed protein encoded by the vaccinia virus A17L gene. J. Virol. **67:**3435–3440.
66. **Rodriguez, J. F., and G. L. Smith.** 1990. Inducible gene expression from vaccinia virus vectors. Virology **177:**239–250.
67. **Rodriguez, J. R., C. Risco, J. L. Carrascosa, M. Esteban, and D. Rodriguez.** 1997. Characterization of early stages in vaccinia virus membrane biogenesis: implications of the 21-kilodalton protein and a newly identified 15-kilodalton envelope protein. J. Virol. **71:**1821–1833.
68. **Rodriguez, J. R., C. Risco, J. L. Carrascosa, M. Esteban, and D. Rodriguez.** 1998. Vaccinia virus 15-kilodalton (A14L) protein is essential for assembly and attachment of viral crescents to virosomes. J. Virol. **72:**1287–1296.
69. **Salmons, T., A. Kuhn, F. Wylie, S. Schleich, J. R. Rodriguez, D. Rodriguez, M. Esteban, G. Griffiths, and J. K. Locker.** 1997. Vaccinia virus membrane proteins p8 and p16 are cotranslationally inserted into the rough endoplasmic reticulum and retained in the intermediate compartment. J. Virol. **71:** 7404–7420.
70. **Sanchez-San Martin, C., T. Lopez, C. F. Arias, and S. Lopez.** 2004. Characterization of rotavirus cell entry. J. Virol. **78:**2310–2318.
71. **Senkevich, T. G., B. M. Ward, and B. Moss.** 2004. Vaccinia virus A28L gene encodes an essential protein component of the virion membrane with intramolecular disulfide bonds formed by the viral cytoplasmic redox pathway. J. Virol. **78:**2348–2356.
72. **Senkevich, T. G., B. M. Ward, and B. Moss.** 2004. Vaccinia virus entry into cells is dependent on a virion surface protein encoded by the A28L gene. J. Virol. **78:**2357–2366.
73. **Sieczkarski, S. B., and G. R. Whittaker.** 2002. Influenza virus can enter and infect cells in the absence of clathrin-mediated endocytosis. J. Virol. **76:** 10455–10464.
74. **Simons, K., and R. Ehehalt.** 2002. Cholesterol, lipid rafts, and disease. J. Clin. Investig. **110:**597–603.
75. **Simons, K., and E. Ikonen.** 1997. Functional rafts in cell membranes. Nature **387:**569–572.
76. **Simons, K., and D. Toomre.** 2000. Lipid rafts and signal transduction. Nat. Rev. Mol. Cell Biol. **1:**31–39.
77. **Smith, G. L., and A. Vanderplasschen.** 1998. Extracellular enveloped vaccinia virus. Entry, egress, and evasion. Adv. Exp. Med. Biol. **440:**395–414.
78. **Sodeik, B., and J. Krijnse-Locker.** 2002. Assembly of vaccinia virus revisited: de novo membrane synthesis or acquisition from the host? Trends Microbiol. **10:**15–24.
79. **Stuart, A. D., H. E. Eustace, T. A. McKee, and T. D. Brown.** 2002. A novel cell entry pathway for a DAF-using human enterovirus is dependent on lipid rafts. J. Virol. **76:**9307–9322.
80. **Sun, X., and G. R. Whittaker.** 2003. Role for influenza virus envelope cholesterol in virus entry and infection. J. Virol. **77:**12543–12551.
81. **Tkachenko, E., and M. Simons.** 2002. Clustering induces redistribution of syndecan-4 core protein into raft membrane domains. J. Biol. Chem. **277:** 19946–19951.
82. **Traktman, P., K. Liu, J. DeMasi, R. Rollins, S. Jesty, and B. Unger.** 2000. Elucidating the essential role of the A14 phosphoprotein in vaccinia virus morphogenesis: construction and characterization of a tetracycline-inducible recombinant. J. Virol. **74:**3682–3695.
83. **Vanderplasschen, A., M. Hollinshead, and G. L. Smith.** 1998. Intracellular and extracellular vaccinia virions enter cells by different mechanisms. J. Gen. Virol. **79:**877–887.
84. **Vanderplasschen, A., E. Mathew, M. Hollinshead, R. B. Sim, and G. L. Smith.** 1998. Extracellular enveloped vaccinia virus is resistant to complement because of incorporation of host complement control proteins into its envelope. Proc. Natl. Acad. Sci. USA **95:**7544–7549.
85. **Van Laethem, F., and O. Leo.** 2002. Membrane lipid rafts: new targets for immunoregulation. Curr. Mol. Med. **2:**557–570.
86. **Wallengren, K., C. Risco, J. Krijnse-Locker, M. Esteban, and D. Rodriguez.** 2001. The A17L gene product of vaccinia virus is exposed on the surface of IMV. Virology **290:**143–152.
87. **Wolffe, E. J., S. Vijaya, and B. Moss.** 1995. A myristylated membrane protein encoded by the vaccinia virus L1R open reading frame is the target of potent neutralizing monoclonal antibodies. Virology **211:**53–63.
88. **Zacharias, D. A., J. D. Violin, A. C. Newton, and R. Y. Tsien.** 2002. Partitioning of lipid-modified monomeric GFPs into membrane microdomains of live cells. Science **296:**913–916.